

The Seismic Fragility Analysis of a Condensate Storage Tank with Age-Related Degradation Considering Realistic Correlations

Young-Sun Choun^{a*}, Min Kyu Kim^a, In-Kil Choi^a, Jinsuo Nie^b, Joseph I. Braverman^b, Charles H. Hofmayer^b
^aIntegrated Safety Assessment Division, Korea Atomic Energy Research Institute, 989-111 Daedeok-daero, Daejeon, 305-353, Republic of Korea

^bEnergy Science & Technology Department, Brookhaven National Laboratory, Upton, NY 11973-5000, USA

*Corresponding author: sunchun@kaeri.re.kr

1. Introduction

The age-related degradation of structures and passive components (SPCs) in nuclear power plants (NPPs) is generally not significant, but it can potentially affect the safety of older plants and become an important factor for their long-term operation.

A seismic fragility analysis of a condensate storage tank (CST) with age-related degradation was investigated in a previous paper [1]. In reality, however, large uncertainties exist in the degradation phenomena of the CST, and there remains no perfect knowledge in representing them. Nevertheless, there is some degree of assurance in the correlations between the degradation cases. This paper shows a stochastic approach to treat age-related degradations in the seismic fragility analysis of a CST.

2. Effect of Degradation on the Fragility of CST

2.1 Condensate Storage Tank

The CST is a flat-bottomed cylindrical tank filled with water under atmospheric pressure. The inner diameter is 50' (15.24 m) and the height (up to the design water level) is 37'-6" (11.43 m). The thicknesses of the shell and bottom plate are 5/8" (16 mm) and about 7 mm, respectively. The CST is made of SA240-304 stainless steel.

The CST is heavily anchored to the reinforced concrete foundation through 78 anchor bolts, which have a diameter of 2-1/2" (63.5 mm) and are A36 steel. The length of the anchor bolts is 3'-6" (1.07 m), with an embedment of about 2'-1" (0.64 m). The anchor bolts were post-installed in pre-formed holes in the concrete foundation using non-shrinking grout. The compressive strength of the concrete foundation of the CST was specified as 4,500 psi. The actual compressive strength of the non-shrinking grout was reported to be 7,550 psi and 111,000 psi, respectively, at 7 days and 21 days [2].

2.2 Fragility Curves for Degraded CST

In this study, three separate degradation cases were considered: (A) degraded stainless tank shell, (B) degraded anchor bolts, and (C) anchorage concrete cracking. The conservative deterministic failure margin (CDFM) method [3] was used for the fragility analysis.

The design basis earthquake (DBE) used for the design of the subject CST was based on NRC Regulatory Guide

1.60 [4] design spectrum anchored to a PGA level of 0.20 g. The initial estimate of the seismic margin earthquake (SME) is set to $1.67 \times 0.2 \text{ g} = 0.334 \text{ g}$ [5]. In developing the fragility curve, aleatory uncertainty, $\beta_R = 0.20$, and epistemic uncertainty, $\beta_U = 0.27$, were used [3].

For a degraded tank shell, the effect of the stress corrosion cracking (SCC) was assumed. Fig. 1(a) shows the mean fragility capacity for a degraded tank shell from 0 up to 60 years. Fig. 1(b) shows that the HCLPF (high confidence low probability of failure) capacity is clearly dominated by sliding until slightly after 45 years, and then by the overturning moment.

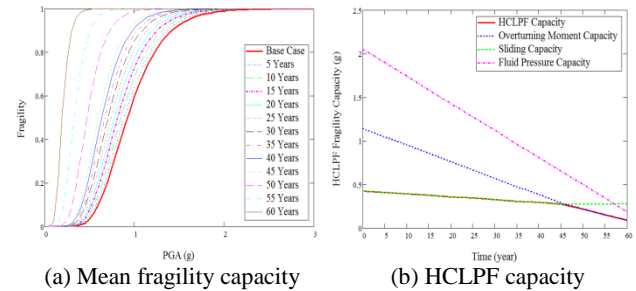


Fig. 1. Mean fragility capacity and HCLPF capacity curves for degraded tank shell

The direct impact of the degraded anchor bolts is simply on the bolt hold down capacity, and consequently on the overturning moment capacity and sliding capacity.

Fig. 2(a) shows the mean fragility capacity of the CST with corroded anchor bolts for a series of years. In a practical sense, it is obvious that the mean fragility is virtually unchanged for a period of 80 years.

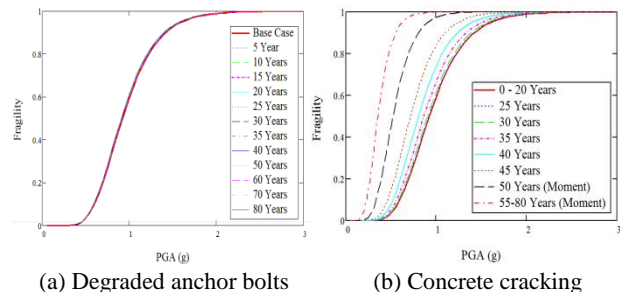


Fig. 2. Mean fragility capacity curves for degraded anchor bolts and anchorage concrete cracking

The impact of concrete cracking is directly on the bolt hold-down capacity, but not the tank shell buckling capacity and fluid pressure capacity; the overturning moment capacity and sliding capacity are affected

consequently. Fig. 2(b) shows that the mean fragility does not change in the first 20 years and in the last 25 years, with an increasing rate of fragility capacity deterioration for the years in the middle.

3. Fragility Analysis with Realistic Correlation between Degradation Cases

3.1 Procedure

For degradation cases A, B, and C, let $A_0(t)$, $B_0(t)$, and $C_0(t)$ be the deterministic degradation models, and the corresponding random models $A(t)$, $B(t)$, and $C(t)$ can be expressed as

$$\begin{aligned} A(t) &= A_0(t) \times a \\ B(t) &= B_0(t) \times b \\ C(t) &= C_0(t) \times c, \end{aligned} \quad (1)$$

where rate factors a , b , and c are random variables with a unit mean and covariance matrix. The use of random processes requires separate realization of the degradation rates at each time step to determine the HCLPF capacity. The simple models as shown in Eq. (1) require much less computation. Once a set of samples is identified for random variables a , b , and c , a sample degradation scenario can be defined.

3.2 Sample Degradation Scenarios

The generated optimum Latin Hypercube samples (LHS) need to be transformed into the correlated rate factors a , b , and c [6]. In this study, the three rate factor random variables are assumed to have lognormal marginal distributions with unit mean and standard deviations of 0.2, 0.25, and 0.3, respectively. The correlation coefficients between (a,b) , (a,c) , and (b,c) are specified as 0.4, 0.4, and 0.7, recognizing that degradations in the anchor bolts and the reinforced concrete foundation have stronger correlation than those involving the stainless steel tank shell.

A total of 11 samples were generated for the rate factors as listed in Table I.

Table I: Sample Rate Factors

| Sample ID | a | b | c |
|-----------|-------|-------|-------|
| 1 | 0.892 | 0.666 | 0.717 |
| 2 | 0.867 | 1.127 | 1.128 |
| 3 | 1.111 | 1.254 | 1.525 |
| 4 | 0.956 | 0.801 | 0.670 |
| 5 | 1.062 | 1.847 | 1.496 |
| 6 | 1.597 | 1.240 | 1.192 |
| 7 | 0.728 | 0.861 | 0.690 |
| 8 | 0.995 | 1.120 | 0.816 |
| 9 | 1.254 | 0.877 | 0.992 |
| 10 | 0.779 | 0.814 | 0.927 |
| 11 | 1.030 | 0.894 | 1.375 |

3.3 Simulation-based Fragility Analyses

Fig. 3 shows various time-dependent HCLPF capacity curves. The thick dotted curve is the average HCLPF capacity at every 5 years, the thick dashed curve is the average year to reach a HCLPF level, and the thick

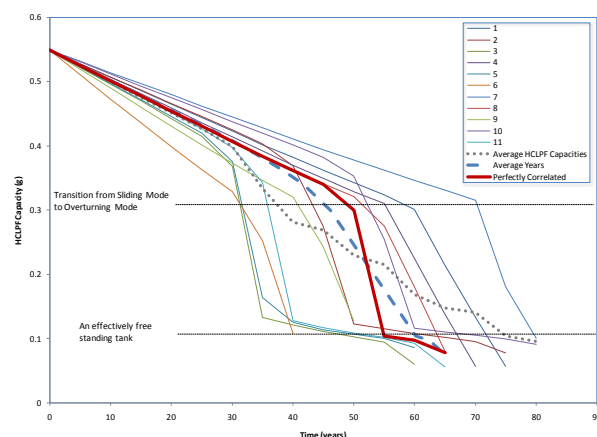


Fig. 3. Simulated HCLPF capacity of CST vs. time

solid curve represents HCLPF capacity with a perfect correlation among the degradation cases A, B, and C.

There are two apparent sharp bends in the curves as indicated by the two horizontal dotted lines. The first bend occurs at a HCLPF level of about slightly higher than 0.3 g, where the controlling mode changes from sliding mode to overturning mode. The second bend occurs at slightly higher than a HCLPF level of 0.1 g, where the CST effectively becomes unanchored. The time for the CST to reach these two HCLPF levels varies significantly among the samples, but generally lies in the range of about 30 to 40 years.

4. Conclusions

The degradation phenomena include large uncertainties. The stochastic approach suggested in this paper can determine the realistic seismic capacity of the CST. Realistic correlations between degradation cases should be considered.

REFERENCES

- [1] Y.S. Choun, M.K. Kim, I.K. Choi, J. Nie, J.I. Braverman, C.H. Hofmayer, The Seismic Fragility Analysis of a Condensate Storage Tank with Age-Related Degradation, Transactions of the Korean Nuclear Society Spring Meeting, 2011, Taebaek, Korea.
- [2] N.H. Lee, I.H. Moon, I.S. Ju, Failure Mechanism for Large-sized Grouted Anchor Bolt under Tensile Load, Proceedings of SMiRT-16, 2001, Washington, D.C.
- [3] R.P. Kennedy, R.C. Murray, M.K. Ravindra, J.W. Reed, J.D. Stevenson, "Assessment of Seismic Margin Calculation Methods," NUREG/CR-5270, U.S. Nuclear Regulatory Commission, Washington, D.C., 1989.
- [4] Regulatory Guide 1.60, "Design Response Spectra for Seismic Design of Nuclear Power Plants," Revision 1, U.S. Nuclear Regulatory Commission, Washington, D.C., 1973.
- [5] SRM on SECY 93-087, "Policy, Technical, and Licensing Issues Pertaining to Evolutionary and Advanced Light-Water Reactor (ALWR) Designs," U.S. Nuclear Regulatory Commission, Washington, D.C., 1993.
- [6] J. Nie, J. Xu, C. Costantino, "P-CARES: Probabilistic Computer Analysis for Rapid Evaluation of Structures," NUREG/CR-6922, U.S. Nuclear Regulatory Commission, Washington, D.C., 2007.